

AD/A-005 401

MODIFICATION OF THE AAD-7 TRACKING
CONTROL SYSTEM AND THE RATE COINCIDENCE
GATE FOR THE AC-130 GUNSHIPS

Edward J. Bauman

Air Force Academy
Colorado

February 1973

DISTRIBUTED BY:

NTIS

National Technical Information Service
U. S. DEPARTMENT OF COMMERCE

Unclassified
Security Classification

AD/A-005401

DOCUMENT CONTROL DATA - R & D

(Security classification of title, body of abstract and indexing annotation must be entered when the overall report is classified)

1. ORIGINATING ACTIVITY (Corporate author) Hq USAFA (Directorate of Faculty Research) USAF Academy, Colorado 80840	2a. REPORT SECURITY CLASSIFICATION Unclassified
	2b. GROUP

3. REPORT TITLE
MODIFICATION OF THE AAD-7 TRACKING CONTROL SYSTEM AND THE RATE COINCIDENCE GATE FOR THE AC-130 GUNSHIPS

4. DESCRIPTIVE NOTES (Type of report and inclusive dates)
Research Report

5. AUTHOR(S) (First name, middle initial, last name)
Lt Colonel Edward J. Bauman

6. REPORT DATE February 1973	7a. TOTAL NO. OF PAGES 46	7b. NO. OF REFS 1
---------------------------------	------------------------------	----------------------

8a. CONTRACT OR GRANT NO.	9a. ORIGINATOR'S REPORT NUMBER(S) 73-2
b. PROJECT NO.	9b. OTHER REPORT NO(S) (Any other numbers that may be assigned this report)
c.	
d.	

10. DISTRIBUTION STATEMENT
Distribution of this document is unlimited

11. SUPPLEMENTARY NOTES	12. SPONSORING MILITARY ACTIVITY Department of Astronautics and Computer Science USAF Academy, Colorado 80840
-------------------------	---

13. ABSTRACT
Two problem areas of the AC-130E gunships were investigated and corrected during deployment to Southeast Asia. Modifications were made to the AAD-7 (forward looking infra-red sensor) tracking control system. These modifications improved the tracking ability of the sensor operator and reduced an undesirable vertical jitter. Modification was also made to the fire control computer program. New equations were programmed to better inhibit firing the guns during high aircraft attitude rates. These high rates would often cause large misses of the ordnance with respect to the target.

Reproduced by
NATIONAL TECHNICAL
INFORMATION SERVICE
U S Department of Commerce
Springfield VA 22151

PRICES SUBJECT TO CHANGE

Unclassified

Security Classification

14.

KEY WORDS

LINK A

LINK B

LINK C

ROLE

WT

ROLE

WT

ROLE

WT

Control Systems
Forward Looking Infra-Red (FLIR)
AC-130E Gunship
Coincidence Gate

ja

Unclassified

Security Classification

MODIFICATION OF THE AAD-7
TRACKING CONTROL SYSTEM AND THE
RATE COINCIDENCE GATE FOR THE
AC-130 GUNSHIPS

by

Lt Colonel Edward J. Bauman

UNITED STATES AIR FORCE ACADEMY

RESEARCH REPORT 73-2

February 1973

Additional copies of this document may be obtained by
writing to the Director of Faculty Research, United States
Air Force Academy, Colorado 80840.

ib

Editorial Review by Captain Jack L. Tinius
Department of English

This Research Report is presented as a competent treatment of the subject, worthy of publication. The United States Air Force Academy vouches for the quality of the research, without necessarily endorsing the opinions and conclusions of the author.

TABLE OF CONTENTS

Abstract. iv
List of Figures v
List of Tables. vi
Acknowledgements. vii
Introduction. 1
Azimuth Gimbal Drive Modification 2
Modification to Reduce Elevation Jitter 5
Results 8
Modification of the Rate Coincidence Gate 12
Appendix A. 17
 Azimuth Modifications 17
 Elevation Modifications 20
Appendix B. 30
Appendix C. 32

ABSTRACT

Two problem areas of the AC-130E gunship were investigated and corrected during deployment to Southeast Asia. Modifications were made to the AAD-7 (forward looking infra-red sensor) tracking control system. These modifications improved the tracking ability of the sensor operator and reduced an undesirable vertical jitter. Modification was also made to the fire control computer program. New equations were programmed to better inhibit firing the guns during high aircraft attitude rates. These high rates would often cause large misses of the ordnance with respect to the target.

LIST OF FIGURES

Figure		Page
1	Azimuth Drive Stabilization.	3
2	Modification to the Azimuth Drive System . .	6
3	Vibrator Isolator Compensation Board	9
4	Vertical IR Displacement on Aircraft 574 . .	10
5	Maximum Expected Miss Due to Coincidence Error with New Coincidence Gate	14
A-1	Azimuth Closed Loop Frequency Response . . .	18
A-2	Gyro Error for a Step Voltage Applied to the Azimuth Servo Amp	21
A-3	Simplified Stabilization Block Diagram . . .	22
C-1	"Time in Coincidence" vs Rate.	33
C-2	Pilot Coincidence Rate vs Time in Coincidence.	35
C-3	Bauman/Kravec "Time in Coincidence" Test	36

LIST OF TABLES

Table		Page
1	Disturbance Transmission to FLIR Platform.	7
A.1	Frequency Responses, $W(s)$ (Closed Loop), for Original and Modified Systems.	27
A.2	Frequency Responses, $G(gs)$ (Open Loop), for Original and Modified Systems.	28
A.3	Frequency Responses, $V(s)$ (Closed Loop), for Original and Modified Systems.	29

ACKNOWLEDGEMENTS

This research was accomplished while the author was attached to the Gunship System Project Office as a technical consultant.

Temporary duty assignment was with the 16th Special Operations Squadron (SOS) Ubon, Thailand. Thanks must go first to those 16th SOS crewmen who pointed out system deficiencies; next to the 8th AMS Forward Looking Infra-Red (FLIR) maintenance personnel who contributed time and facilities to perform numerous ground tests. Finally, appreciation is expressed to the Texas Instrument Company technical representatives who assisted in all FLIR tests and without whom it would have been impossible to complete the investigation and make the necessary modifications. Similar appreciation must be expressed to Capt John Kravec, Gunship Project Office, for his software expertise in programming the modification to the rate coincidence gate.

INTRODUCTION

Operators often reported poor performance when tracking with the AAD-7 Forward Looking Infra-Red (FLIR) sensor. Evaluation of Bomb Damage Assessment (BDA) films showed that two problems were evident with the tracking capability of this sensor. First, the average operator could not track a target and keep it centered consistently on his scope to within the desired 0.5 milliradian (m.r.) accuracy. Second, a vertical jitter was present at a frequency of about 10 to 15 HZ and varied in peak amplitude between plus and minus 0.25 to 1.0 m.r. Some sets were more susceptible to vibration and as a result had jitter with the larger peak amplitude. This jitter would build to its peak amplitude and then diminish aperiodically.

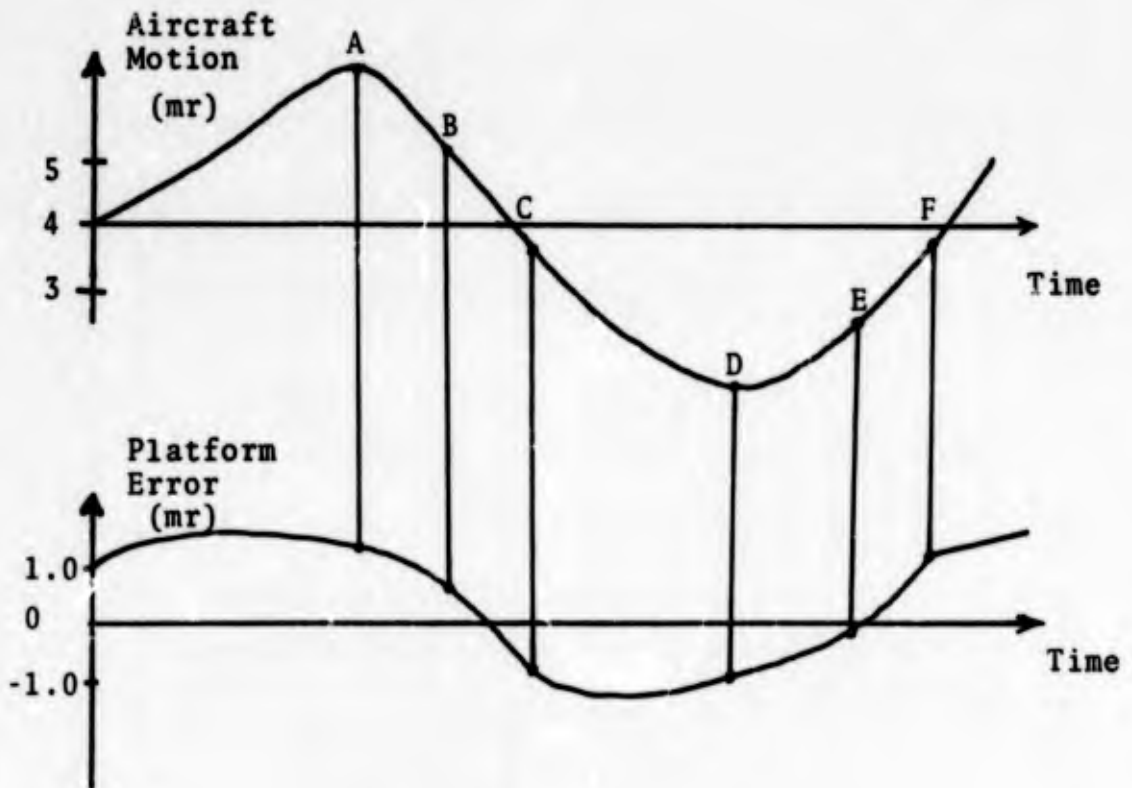
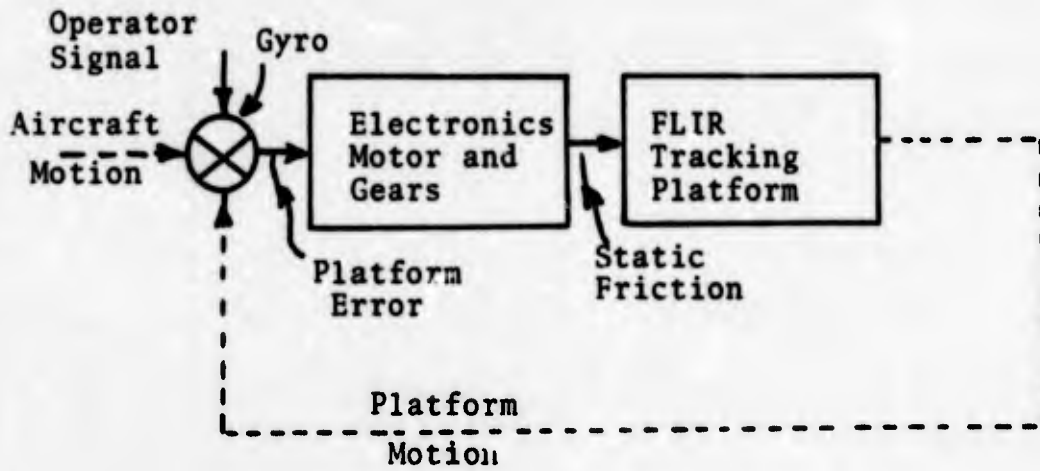
The tracking accuracy problem directly affects the system accuracy, because wherever the sensor is pointing is the assumed target position. Tracking 1 m.r. off the target introduces a 1 m.r. impact error. The jitter problem makes target detection, identification, and resolution more difficult. It also adds to the tracking problem since the sensor operator

must attempt to track the center of a bouncing target image.

AZIMUTH GIMBAL DRIVE MODIFICATION

Tests in the FLIR maintenance shop showed that an azimuth stabilization gyro error (i.e., a tracking error) of between 0.5 to 1.5 m.r. had to be developed to overcome the static friction of the gear assembly and cause drive assembly movement. The amount of static friction is a function of gear loading; the more loading the more friction. However, gear loading is necessary to eliminate gear backlash effects which would cause the drive system to oscillate. Therefore, a system modification had to be found to produce enough torque to overcome this loading for smaller gyro errors.

Before discussing the solution to this problem, let's discuss why this error causes tracking difficulties. Figure 1 shows a simplified block diagram of the azimuth stabilization system. As the aircraft moves in azimuth, the platform is moved and the angular platform error is measured by the gyro. This error is amplified by the electronics and fed to the motor which drives the platform to counter the aircraft motion. An arbitrary aircraft motion is also shown



Azimuth Drive Stabilization

Figure 1

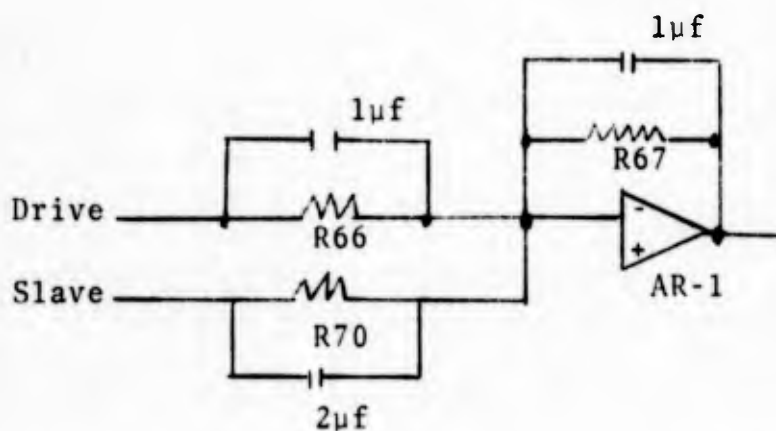
in Figure 1 along with the resulting platform error. At point A the aircraft is not moving with respect to the target, so the platform error is just that which was needed to overcome static friction when the aircraft was moving in a positive direction. However, when the aircraft begins moving in a negative direction and carries the platform with it through point B and to point C where enough error has been generated to overcome the static friction in the negative direction, a slight amount more error is needed to drive the platform to counter the negative aircraft rate. The process is repeated at D, E, and F and at any other time the aircraft changes direction. In this example the sensor operator sees at least a 2 m.r. movement of the target image when this platform motion occurs. He is then obligated to correct the movement by applying an operator signal via his hand controller.

A simple way to solve this problem would be to increase the electronic gain so that a smaller platform error produces the needed torque to overcome static friction. However, if the gain is increased appreciably, the closed loop system becomes unstable. Therefore a lag compensation network was selected (See Appendix A) to increase the low frequency gain and

still maintain stability. Figure 2 shows the compensation network that increased the low frequency gain by nearly ten times and thus reduced the platform error due to static friction by nearly a factor of ten. The only modifications were changing the values of R-66, R-67, and R-70 and paralleling them with capacitors. The slave circuit input had to be changed merely to nullify the capacitor-resistor combination across AR-1. Therefore, the slave circuit behavior remains unchanged.

MODIFICATION TO REDUCE ELEVATION JITTER

The problem just discussed for azimuth static friction did not seem to produce appreciable errors in the elevation platform position. However, aircraft vibrations introduced a 10 to 15 HZ oscillation that at first was thought to be directly attributed to the 13 HZ natural frequency of the rubber vibration isolator mounts. These mounts which attach the FLIR to the aircraft were subsequently replaced by solid metal mounts for a test flight on aircraft AC-130A/029. The jitter became even more random and severe during this test. Also, higher frequency vibrations were transmitted through the solid mounts, causing a slight blurring of



Note: AR-1 is the existing operational amplifier on the 1A11 printed circuit board.

R-66 is changed to 100K ohms

R-67 is changed to 1.0 meg ohms

R-70 is changed to 510K ohms

The capacitors are added as shown.

Modification to the Azimuth Drive System

Figure 2

the scope image presentation; therefore, the rubber mounts were retained.

The logical remedy for this jitter was to increase the frequency response of the elevation system to electrically drive the platform and cancel the detected vibrations. This modification proved to be a difficult design problem which is described in Appendix A. The designers of the AAD-7 gimbal electronics and mount assisted in this project. The task could not have been completed without their expert help.

Appendix A shows theoretically that disturbance frequencies in the jitter range are reduced by the amounts shown in Table 1. Note the reduction of the output to about 50 percent of its original value with the modified system at the offending frequencies, 10 to 15 HZ.

Frequency (HZ)	Disturbance: Output/Input		Disturbance Output Modified/Original
	Original	Modified	
5.0	0.70	0.25	0.35
10.0	1.20	0.50	0.40
15.0	1.30	0.75	0.60
20.0	(1.2)*	3.0	2.5

*Estimated

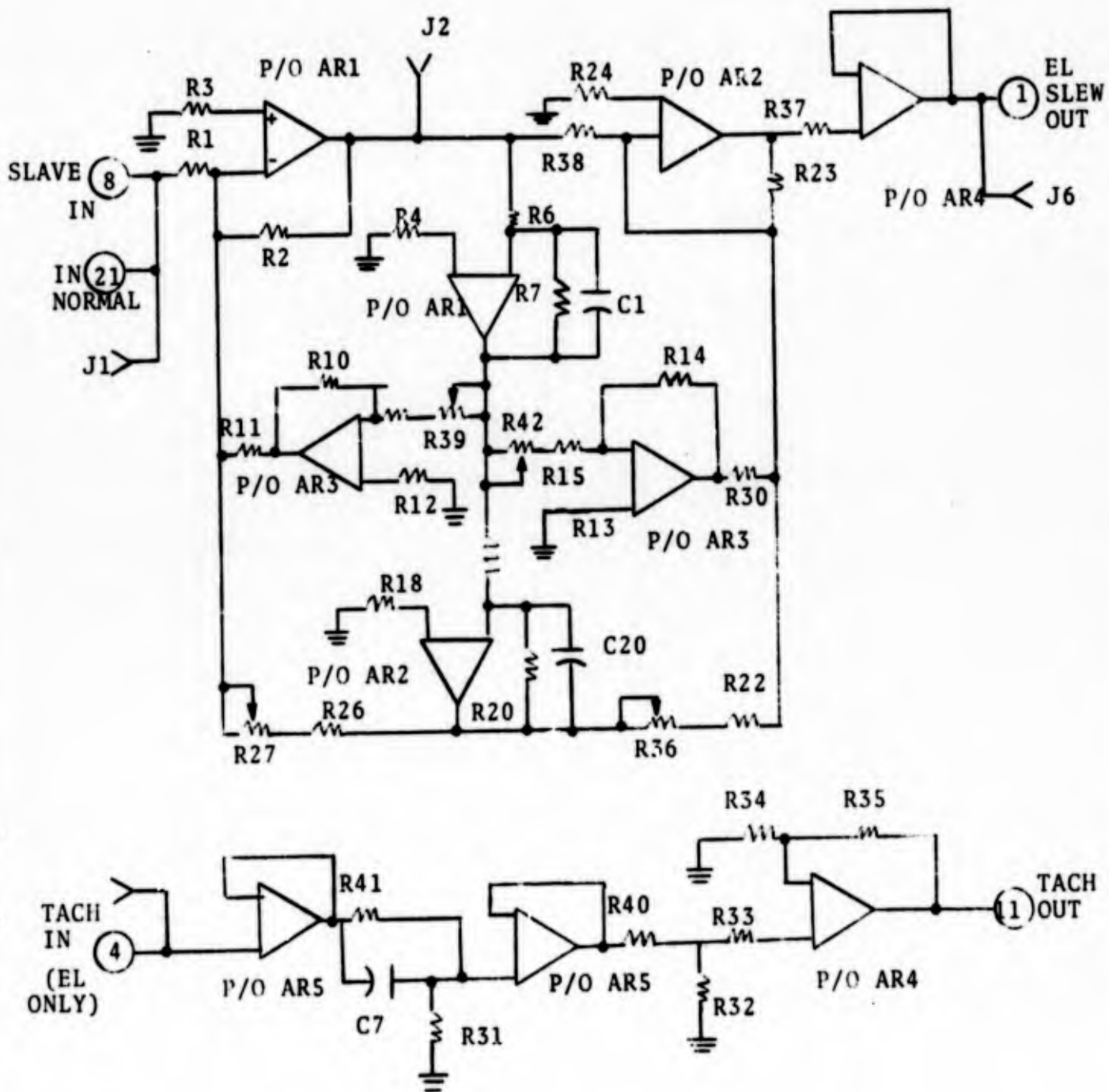
Disturbance Transmission to FLIR Platform

Table 1

At 20 HZ, unfortunately, the gain of the modified system is high and the phase reinforces the disturbance. Fortunately, this frequency is higher than the frequency of most large amplitude disturbances. Also, the rubber vibration isolators help damp these higher frequencies. Figure 3 is a schematic of the vibration isolator board which was modified. A 0.82 μ .f. capacitor was added across R1. The adjustments of potentiometers were changed to read as follows: R36=4.1K; R27=R39=R42=0. The tachometer was completely disconnected from the circuit by opening its path just after the TACH! OUT point as it feeds into the next circuit board.

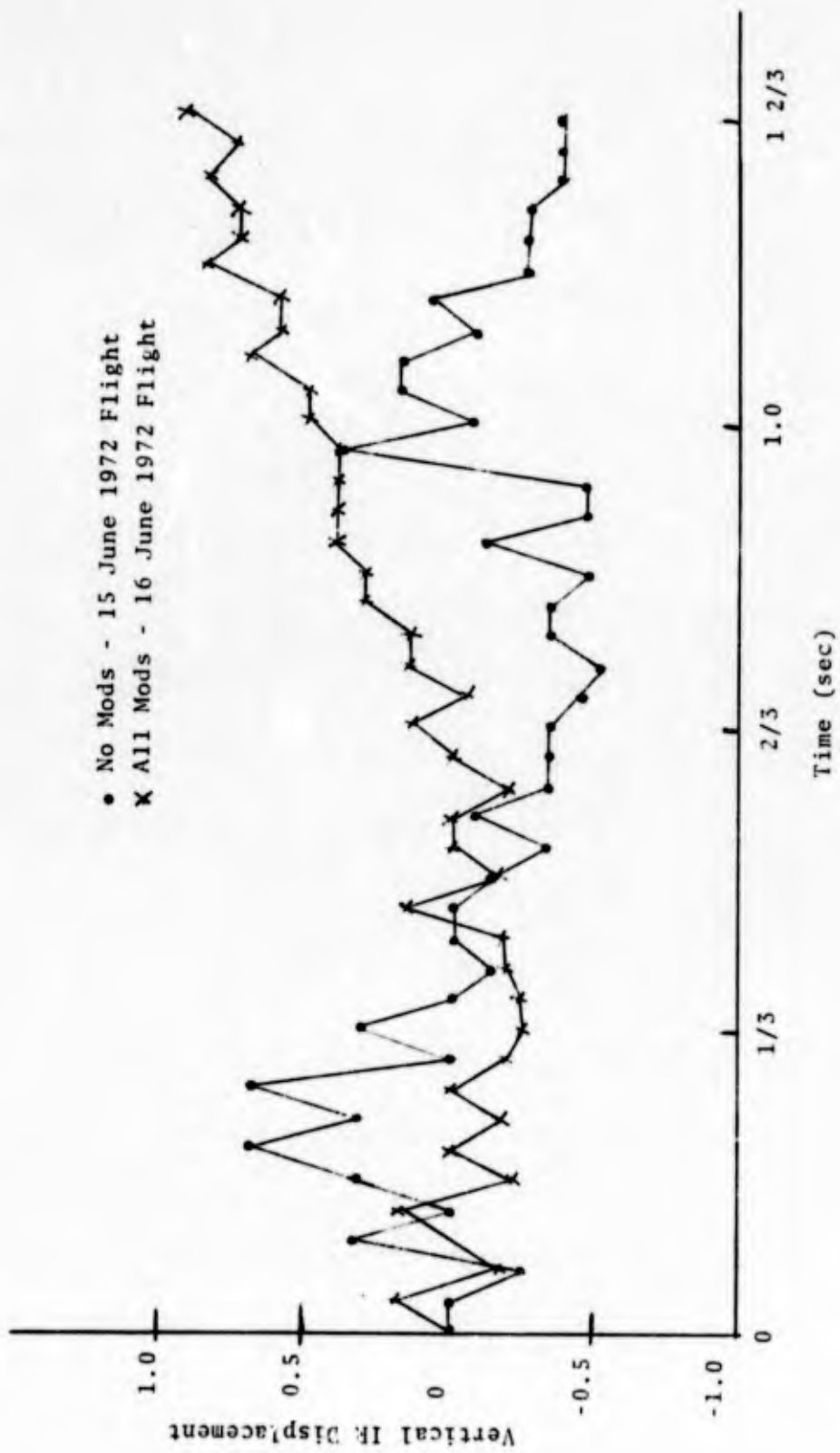
RESULTS

The results were documented by producing film of BDA (Bomb Damage Assessment) tape. This method gives only a semi-quantitative evaluation of the reduction in jitter. Because the IR system produces only 30 picture frames/sec, it is difficult to measure 10 to 15 HZ oscillations. Picture resolution and the measurement method gave measurement accuracy no better than 0.25 m.r. Figure 4 shows the results of an attempt to measure this jitter with and without the jitter modifications.



Vibration Isolator Compensation Board

Figure 3



Vertical IR Displacement on Aircraft 574

Figure 4

The disc recorder playback at the BDA facility was used to measure displacement of the IR image at each frame (each data point represents one frame; i.e., 1/30 sec.). The jitter here is directly related to the frame frequency since it merely samples the jitter frequency. However, the maximum excursions between points with the modifications is never more than ± 0.25 m.r. while without the modifications the jitter excursions approach ± 0.5 m.r. The build up and subsequent decay of the jitter can be seen in both cases.

The ideal way to have measured the jitter would have been to install an airborne high speed instrumentation recorder. The output of the gyro could then have been recorded to give a direct measure of the jitter. Unfortunately, a recorder of this type was not available at Ubon, RTAFB. It is recommended that this measurement test be performed at Hurlburt Field, Fla., with and without the jitter modifications.

The BDA tape gives a very accurate measure of overall tracking accuracy. Appendix B lists 20 seconds of tracking data by the AAD-7 mounted in aircraft 574. The tracking was done on the boresight building during airborne sensor alignment prior to the 19 June 1972 mission. At this time both the azimuth and

elevation modifications had been made to this FLIR sensor. From the mean tracking point on the building, the standard deviation was just less than 0.25 m.r. in both axes. Thus, for this test, the root of the sum of the squares (R.S.S) is just 0.35 m.r. or within the desired 0.5 m.r.

In conclusion, the tracking accuracy now appears to be within desired limits. However, the elevation jitter was not eliminated. It was reduced significantly, but realistically plus or minus 0.2 m.r. may not be an uncommon peak amplitude in some sets.

MODIFICATION OF THE RATE COINCIDENCE GATE

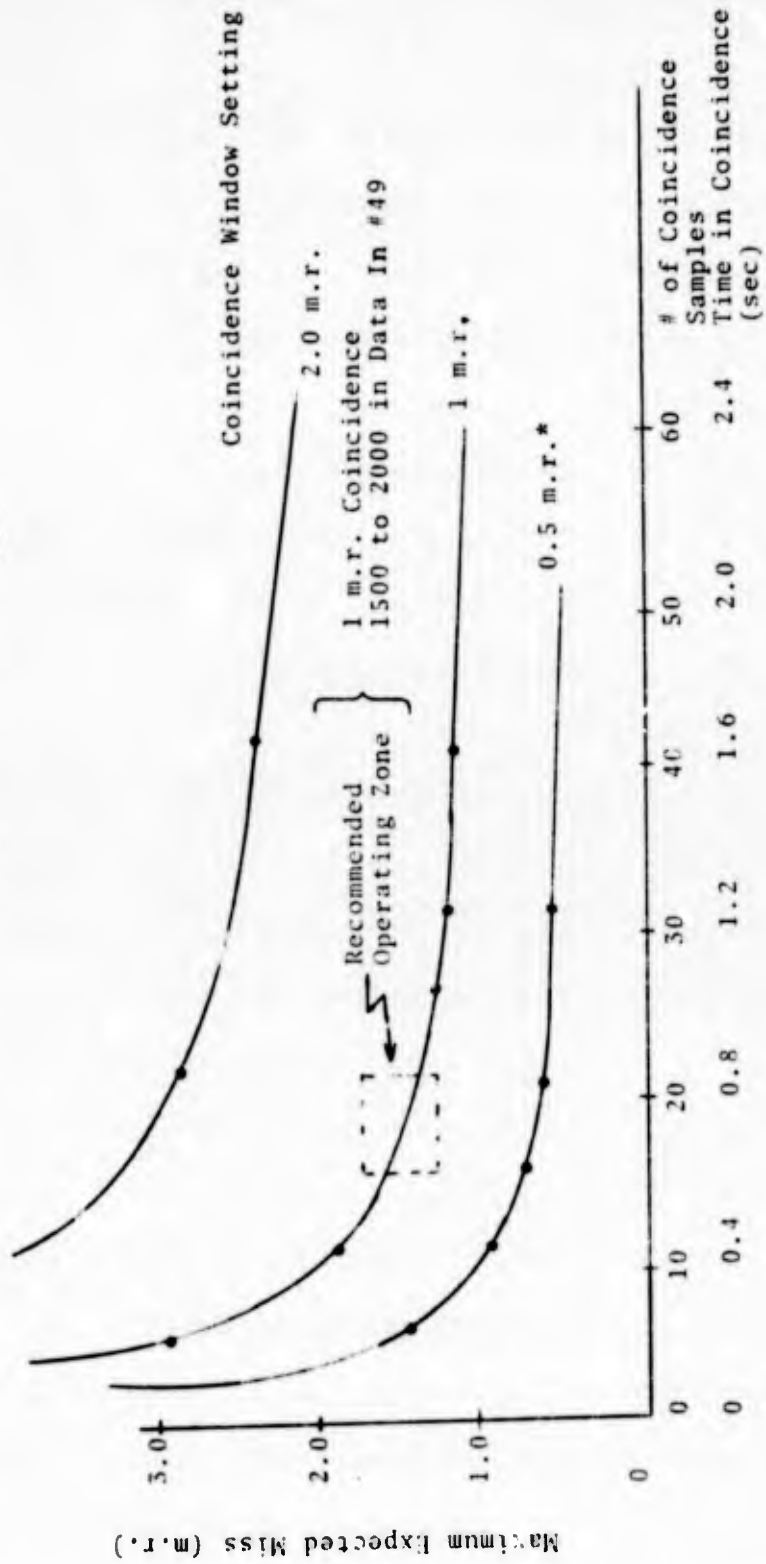
Difficulty was experienced with the rate coincidence gate. This gate is a test of how fast the C.I.P. (computed impact point) is moving with respect to the P.A. (primary aim line to the target). If the radial distance between the two is less than the coincidence setting (window), then the rate of movement of this radial distance is also checked. If this rate is less than the rate gate setting, the computer will only then allow the firing pulse to be initiated.

This rate gate seemed to work well during the Pave Aegis tests at Eglin in Jan-Feb 72. In fact, test data showed the pilot error (difference between the

P.A. and C.I.P.) was significantly reduced when the rounds were fired. However, operational use showed that shots were often fired with excessive rate compared to the rate gate setting. Therefore, a new coincidence gate was devised to keep the pilot error less than the coincidence setting for a specified time. For example, if the navigator set computer "DATA IN" Instruction No. 49 at a setting of 2000, the pilot had to remain in coincidence for 21 minor computer computation cycles or 0.8 seconds. Effectively then, he must stop the rate so as to be in coincidence for that period. Psychologically he gears himself to keeping his "sights" in coincidence rather than just reducing the rate of movement. This new attitude and new "time in coincidence" gate worked very successfully.

Figure 5 shows the maximum expected 105mm miss for a given time in coincidence. Appendix B gives a derivation of the curves in this figure. Combat missions showed that a 1 m.r. coincidence window with coincidence being maintained from 0.5 to 0.8 sec (setting of 1500 to 2000) allowed the pilot to consistently get off shots without excessive pilot error.

Figure 5
 Maximum Expected Miss Due to Coincidence Error
 with New Coincidence Gate
 (105mm)



Maximum Expected Miss Due to Coincidence Error
 with New Coincidence Gate
 (105mm)

Figure 5

* At 00 in coincidence window (approx 0.5 m.r.) a setting of 5.00 or less was necessary for the pilot to be able to shoot the gun consistently.

However, since it is somewhat demanding for a pilot to hold coincidence for a long period when it is really only rate that needs to be reduced, another revised rate gate was sent to Ubon by IBM. This new gate again does not consistently inhibit "rated" shots. I therefore strongly recommend the "time in coincidence" test to be used since it has proven itself during combat missions. Appendix C gives the flow diagram and software code as programmed by Captain John Kravec which was handloaded in software program GS-26-6.

LIST OF REFERENCES

1. DiStefano, Stubberud and Williams, Feedback and Control Systems. New York, McGraw-Hill Book Co., 1967.

APPENDIX A

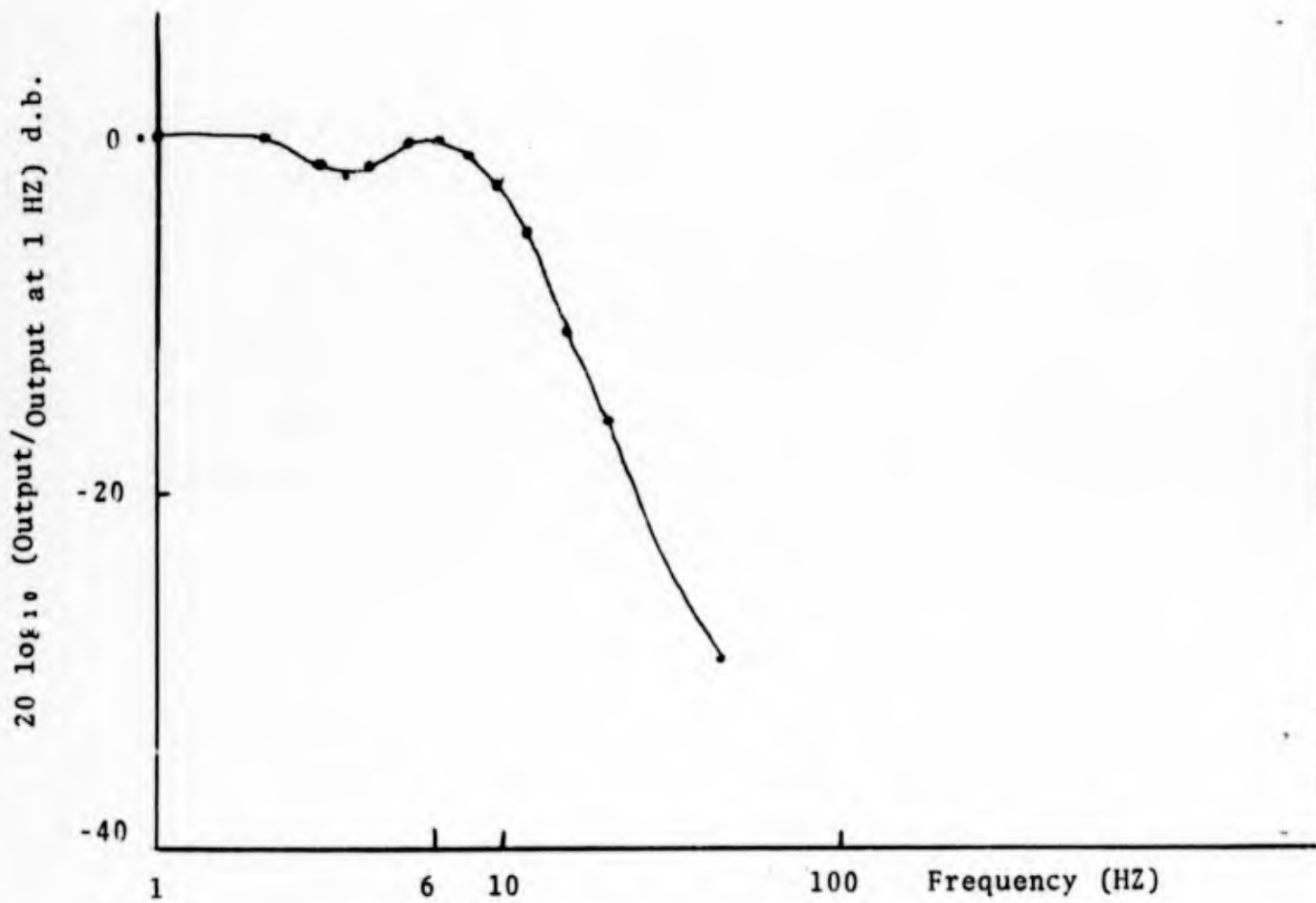
AAD-7 Gimbal Electronics Modification

AZIMUTH MODIFICATIONS

Figure A-1 shows the experimental closed loop frequency for the azimuth drive system. A sinusoidal signal was fed to the input of the servo amplifier and the output measured at the output of the demodulator board. Since the output below 1 HZ was essentially constant, the output at 1 HZ was used as the reference value. The system peaks at about 6 HZ. This means that the zero d.b. crossover of the open loop response is at about 6 HZ. Therefore, a lag compensation circuit must have its lag break frequency well below 6 HZ. Reference 1 shows that if the lag break is a factor of 40 below a given frequency only about -13 degrees phase shift is added at that frequency for a d.c. gain factor of 10. The lag break frequency was chosen as: $f_{lag} = 0.16$ HZ. Using the gain factor of 10, the lead break occurs at $f_{lead} = 1.6$ HZ. The transfer function for the lag compensation in Figure 2 is given by:

$$TF_{lag} = \frac{s + \omega_b}{s + \omega_a}$$

where



Azimuth Closed Loop Frequency Response

Figure A-1

$$\omega_b \equiv 2\pi f_{lead} = 10$$

$$\omega_a \equiv 2\pi f_{lag} = 1$$

However, for any RC parallel combinations, the break frequency (in radians) is given by

$$\omega = \frac{1}{RC}$$

since in both cases a $1\mu f$ capacitor has been chosen we can solve for R:

$$\omega_b = \frac{1}{R(1 \times 10^{-6})} = 10 \text{ or } R \equiv R66 = 1 \times 10^5 \text{ ohms}$$

$$\omega_a = \frac{1}{R(1 \times 10^{-6})} = 1 \text{ or } R \equiv R67 = 1 \times 10^6 \text{ ohms}$$

To maintain an original slaving gain, R70 was increased to 510K and the $2\pi f$ capacitor added to give a ω_{lead} , for the slave input, of unity which just cancels the ω_{lag} . Thus, the slave circuit behavior is unchanged.

The added -13° degrees phase shift previously mentioned forces the open loop gain to be reduced somewhat below the added factor of 10 so a good stability margin can be maintained.

Note that with the static friction, the system behaves open loop until the friction is overcome. The one second time constant of the lag now allows rapid movements of the aircraft to "drag" the platform back toward its stabilized position. This

phenomenon is evident when the test step generator is used to set the proper azimuth gain. The resulting gyro error is now as shown in Figure A-2. Also shown is the error without the modification. The steady state improvement is clearly evident. Note that the sensor operator will similarly see an initial movement of the image as the aircraft changes direction (see also Figure 1). However, with the modification the image returns to near its stabilized position in a few tenths of a second, so no correction needs to be made by the operator.

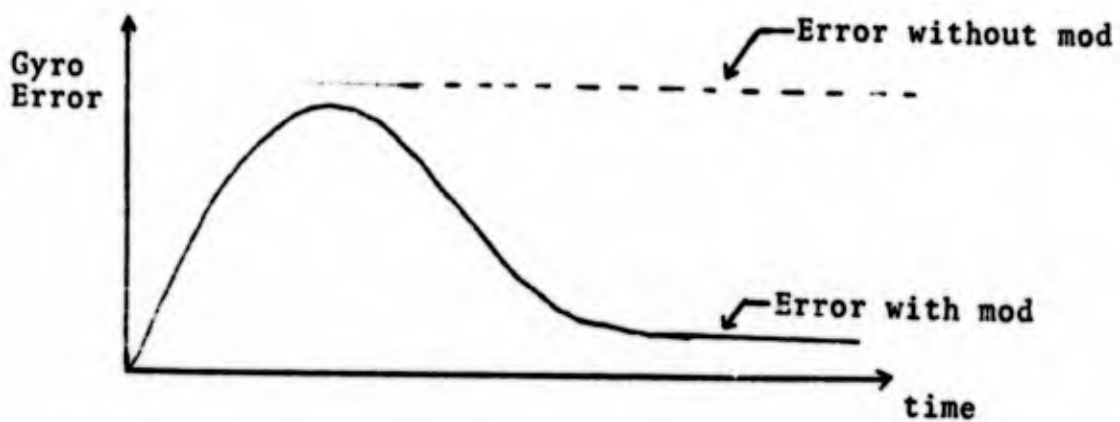
ELEVATION MODIFICATIONS

The following analysis shows that a tachometer is not desirable for stabilizing a system to an inertial reference position. Figure A-3 shows a simplified block diagram of the stabilization system.

$\psi_{P/I}$ is the platform motion with respect to an inertial reference. This is the motion that needs to be made as small as possible. It is easy to show that:

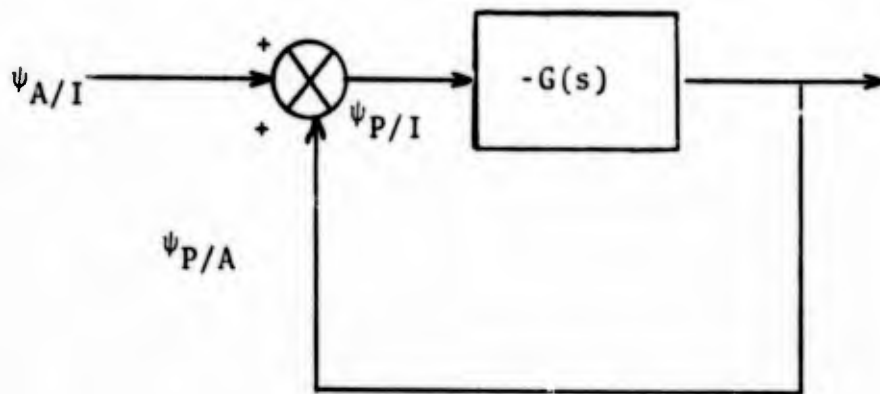
$$\psi_{P/I} = \left[\frac{1}{1+G(s)} \right] \psi_{A/I} \quad (A.1)$$

In this case $\psi_{A/I}$, the aircraft motion tends to move the platform position. If the bracketed term can be made small, then $\psi_{P/I}$ will be small.



Note: Gyro error is proportional to stabilized IR platform position error.

Gyro Error for a Step Voltage
Applied to the Azimuth Servo Amp
Figure A-2



Where: $\psi_{P/I}$ = I.R. Platform angular motion with respect to an Inertial reference.

$\psi_{P/A}$ = I.R. Platform angular motion with respect to the aircraft.

$\psi_{A/I}$ = Aircraft angular motion with respect to an Inertial reference.

$G(s)$ = Transfer function of the gyro, stabilization electronics, motor, gears and platform.

Simplified Stabilization Block Diagram

Figure A-3

With a tachometer and assuming a simple second order system [the analysis is valid for a higher order system was well], $G(s)$ is given by

$$G(s) = \frac{K}{s(Js+b+K_J K_M)} \quad (A.2)$$

where: K is a gain term of the entire system.

J is the moment of inertial of the mechanical system.

b is the viscous damping of the mechanical system.

K_M is the gain of the servo amp and motor.

K_T is the tachometer feedback gain.

Substituting (A.2) in (A.1) we have

$$\psi_{P/I} = \left(\frac{b+K_T K_M}{K} \right) \left[\frac{\tau_1 s + 1}{\omega^2 s^2 + 2\zeta_1 \omega_1 s + 1} \right] (s\psi_{A/I}) \quad (A.3)$$

where τ_1, ζ_1 , and ω_1 are functions of the previous terms.

With a forward loop lead circuit instead of tachometer feedback, $G(s)$ is given by

$$G(s) = \frac{K(\tau s + 1)}{s(Js + b)} \quad (A.4)$$

where τ is the lead time constant.

Substituting (A.4) into (A.2) we have

$$\psi_{P/I} = \left(\frac{b}{K} \right) \frac{(\tau_2 s + 1)}{\omega_2^2 s^2 + 2\zeta_2 \omega_2 s + 1} (s\psi_{A/I}) \quad (A.5)$$

where τ_2, ζ_2 , and ω_2 are functions of previous terms.

For a constant rate input; i.e., $(s\psi_{A/I}) \equiv M$, the steady state error from (A.3) is found by setting

$s=0$, giving

$$(\psi_{P/I})_{ss} = \left(\frac{b + K_T K_M}{K} \right) M \quad (A.6)$$

The steady state error from (A.5) is given by

$$(\psi_{P/I})_{ss} = \left(\frac{b}{K} \right) M \quad (A.7)$$

Thus, the steady state error with the tachometer, (A.6), is increased by a factor of $\frac{K_T K_M}{K}$ when compared to the lead circuit, (A.7). It seems desirable to replace the tachometer by a lead circuit which was done by opening the tachometer circuit and replacing it by the capacitor across R1 (Figure 3). Equations (A.6) and (A.7) also show that K directly reduces the error. However, if K becomes too large, the system becomes unstable. In fact, the basic reason for the tachometer or the lead is to be able to increase K and keep the system stable. It was found that just the lead circuit, as described, could not maintain K high enough to appreciably decrease platform vibration errors. The Texas Instrument Company technical representative found that he could readjust potentiometers on the vibration isolation board to appreciably give more lead, therefore K could be increased. Further, the lead helped to reduce the magnitude of the bracket term of (A.1) in the jitter frequency range.

A frequency response of the system was made by inserting a sinusoidal voltage at the input to the servo amp. The output was measured from the system just before the input to the servo amp. As a result the measured closed loop frequency response for the transfer function was:

$$W(s) \equiv \frac{G(s)}{1+G(s)} \quad (\text{A.8})$$

The frequency response of the original system (with tachometer) and of the modified system were both measured. Table A.1 shows the results. Unfortunately, adequate equipment for precise measurements was not available, and the values are approximate. Especially after the modification was made, equipment was no longer available to adequately measure phase; therefore, only a few measurements were made. Note that the lead has greatly reduced the negative phase shift and thus extended the bandwidth.

However, $W(s)$ is not the transfer function desired. Rather, from (A.1) we need to determine

$$V(s) \equiv \frac{1}{1+G(s)} \quad (\text{A.9})$$

Using a Nichols Chart (reference 1), $G(s)$ can graphically be determined by plotting $W(s)$. Then $V(s)$ can

be determined analytically since $s=j\omega$ for a frequency response test.

Frequency HZ	Original System		Modified System	
	Output/Input	Phase	Output/Input	Phase
2	1.0	-55°	1.0	small
5	0.6	-110°	1.0	-15°
10	0.2	-145°	1.0	-30°
15	0.4	-130°	1.0	-45°
16	0.2	-180°	Not measured	
20	Not measured		2.5	-160°
25	Not measured		2.0	-200°
30	Not measured		1.0	-230°
35	Not measured		1.0	-270°
40	Not measured		0.5	-270°

Frequency Responses, $W(s)$ (Closed Loop),
for Original and Modified Systems

Table A.1

Frequency HZ	Original System		Modified System	
	Output/Input	Phase	Output/Input	Phase
2	1.1	-118°		
5	0.5	-138°	4.0	-96°
10	0.2	-150°	2.0	-105°
15	0.3	-143°	1.3	-112°
16	0.2	-180°		
20			0.65	-175°
25			0.65	-188°
30			0.6	-203°
35			(0.7)?	-222°
40			0.4	-242°

Frequency Responses, G(s) (Open Loop),
for Original and Modified Systems

Table A.2

Frequency (HZ)	Magnitude of $V(s) \equiv V(s) $	
	Original	Modified
2	0.70	—
5	0.70	0.25
10	1.20	0.50
15	1.30	0.75
16	1.25	—
20	—	3.0
25	—	3.0
30	—	2.0
35	—	—
40	—	1.1

Frequency Responses, $|V(s)|$ (Closed Loop),
for Original and Modified Systems

Table A.3

APPENDIX B

AAD-7 Tracking-Boresight Bldg.
19 June 1972 (AC-130E/574)

Time (sec)	AZ (mr)	EL (mr)	Time (sec)	AZ (mr)	EL (mr)
0	0	0	5.2	-.25	0
.2	-.25	0	5.4	-.25	0
.4	-.25	0	5.6	-.25	0
.6	-.25	0	5.8	-.25	0
.8	-.25	0	6.0	-.25	0
1.0	-.25	.25	6.2	-.25	-.5
1.2	-.25	.25	6.4	-.25	-.25
1.4	-.25	.25	6.6	-.25	0
1.6	-.25	0	6.8	0	0
1.8	-.25	0	7.0	.25	.25
2.0	-.25	0	7.2	.25	0
2.2	0	0	7.4	.25	0
2.4	0	0	7.6	.25	0
2.6	-.25	0	7.8	.5	.25
2.8	-.25	0	8.0	.25	.25
3.0	-.25	-.5	8.2	.25	0
3.2	-.25	-.25	8.4	.25	-.25
3.4	-.25	0	8.6	.25	-.25
3.6	-.50	0	8.8	.25	-.25
3.8	-.25	0	9.0	0	0
4.0	-.25	0	9.2	0	0
4.2	-.25	0	9.4	-.25	0
4.4	-.50	.25	9.6	-.25	-.5
4.6	-.25	.25	9.8	-.25	0
4.8	-.25	.25	10.0	-.25	-.25
5.0	-.25	.25			
10.2	-.25	-.25	15.2	-.5	-.5
10.4	-.25	0	15.4	-.25	-.5
10.6	-.25	0	15.6	0	-.25
10.8	-.25	.25	15.8	-.25	0
11.0	0	0	16.0	-.25	0
11.2	-.25	0	16.2	-.25	0
11.4	-.25	0	16.4	-.25	0
11.6	-.25	0	16.6	-.25	-.5
11.8	-.25	0	16.8	-.5	-.5
12.0	-.25	0	17.0	-.25	-.5
12.2	-.25	0	17.2	-.25	0
12.4	-.25	.25	17.4	-.25	0
12.6	-.50	.25	17.6	-.25	.25

Time (sec)	AZ (mr)	EL (mr)	Time (sec)	AZ (mr)	EL (mr)
12.8	-.25	0	17.8	-.25	0
13.0	-.5	.25	18.0	-.25	0
13.2	-.5	-.25	18.2	0	0
13.4	-.5	-.25	18.4	.25	-.25
13.6	-.5	-.5	18.6	.25	-.25
13.8	-.5	0	18.8	0	-.5
14.0	-.5	0	19.0	0	-.5
14.2	-.5	0	19.2	0	-.5
14.4	-.75	-.5	19.4	0	-.5
14.6	-.75	-.5	19.6	0	-.25
14.8	-.5	-.5	19.8	-.25	0
15.0	-.75	-.5	20.0		

Azimuth Mean -0.2 m.r.
 Elevation Mean -0.1 m.r.
 Azimuth Standard Deviation 0.25 m.r. $\equiv \sigma_{AZ}$
 Elevation Standard Deviation 0.25 m.r. $\equiv \sigma_{EL}$

$$\sigma_T = (\sigma_{AZ}^2 + \sigma_{EL}^2)^{1/2} \approx 0.35 \text{ m.r.}$$

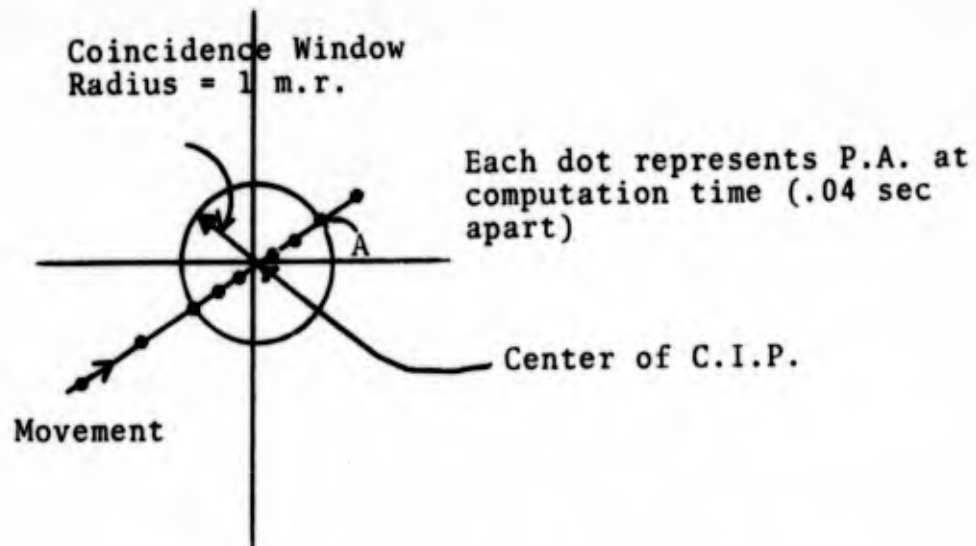
APPENDIX C

"Time in Coincidence" Test

When the computer gives the firing pulse, it takes about 0.2 sec before the 105mm shell leaves the gun barrel, and it takes about 0.35 sec for the 40mm. If the P.A. is moving at a rate of 18 m.r./sec (about 1 deg/sec) with respect to the C.I.P. then by the time the 105mm leaves the barrel the P.A. will have moved 3.6 m.r. for the 105mm and 6.3 m.r. for the 40mm. If the C.I.P. and P.A. were perfectly in coincidence when the firing pulse was given, then the above quoted movements would be the misses for the respective rounds. Thus, we see that allowing the fire pulse to be initiated only for low pilot error rates is very important to increase system accuracy.

"Time in coincidence" can be correlated to maximum rate by the following argument. Figure C-1 shows a 1 m.r. coincidence window (2 m.r. in diameter). If the pilot stays in coincidence for 0.4 seconds and passes through the diameter (maximum distance) then the maximum rate he could have is

$$\frac{2 \text{ m.r.}}{0.2 \text{ sec}} = 10 \text{ m.r./sec}$$



"Time in Coincidence" vs Rate

Figure C-1

Figure C-2 shows a plot of rate vs time in coincidence using this calculation for various coincidence windows (105mm).

Again looking at Figure C-1, if the time in coincidence was set at 0.2 seconds (5 sample intervals), the firing pulse would be initiated at point A. Then 0.2 sec later the gun (105mm) would fire. At this time the P.A. would have traveled*

$$(0.2) \times (10 \text{ m.r./sec}) = 2 \text{ m.r.}$$

However, the P.A. was already 1 m.r. from the C.I.P. at point A, therefore the maximum expected miss is

*Assumes rate remains constant

3 m.r. By using this reasoning the following formula is deduced for maximum expected miss:

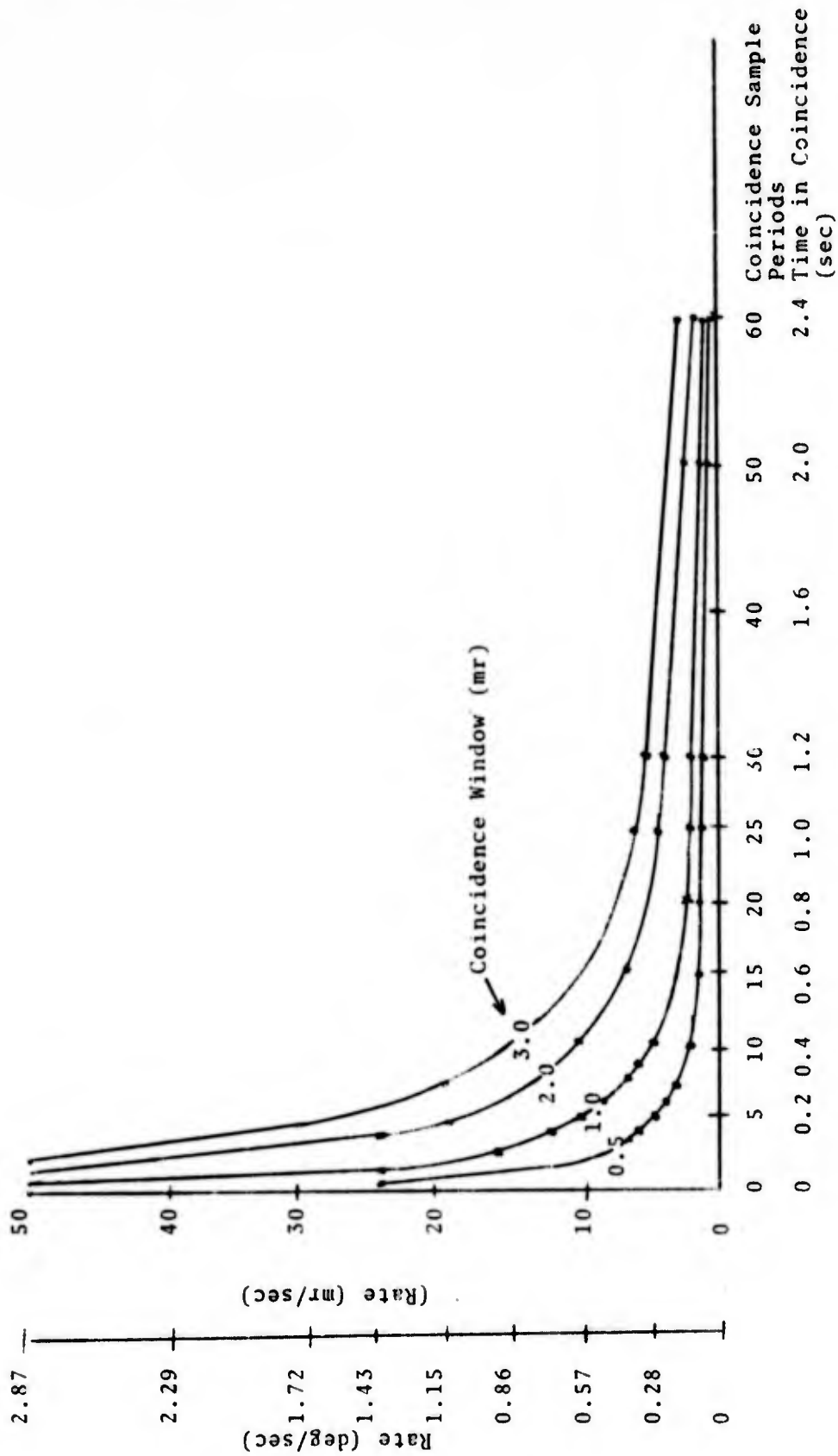
$$\text{Maximum Miss in m.r.} = \frac{2R}{.04N} T_d + R$$

where R = radius of coincidence window (m.r.)

N = number of sample intervals (samples)

T_d = Time delay between firing pulse and round leaving barrel

Figure 5 shows a plot of this maximum expected miss. Figure C-3 shows the flow diagram and software program to implement the time in coincidence test.



Pilot Coincidence Rate vs Time in Coincidence

Figure C-2

Handloads to GS-26-6

3F5A	C044	SRDA 4
B	69DA	S EPS
C	5942	STA TWEPOO
D	2605	BFNP**5
E	0500	ZQ
F	0600	XAQ
3F60	5FFB	STA CNT
1	7F85	LD EPSR
2	2707	BF**7
3	EFFB	TALLY CNT
4	7FFB	LD CNT
5	0500	ZQ
6	C0C9	SLD 9
7	6F85	S EPSR
8	3408	BBM**8
9	7942	LD TWEPOO
3F6A	1900	BIA 'O'
35EA	0000	NOP
35EB	5C01	STA LCCG

CHECKSUM

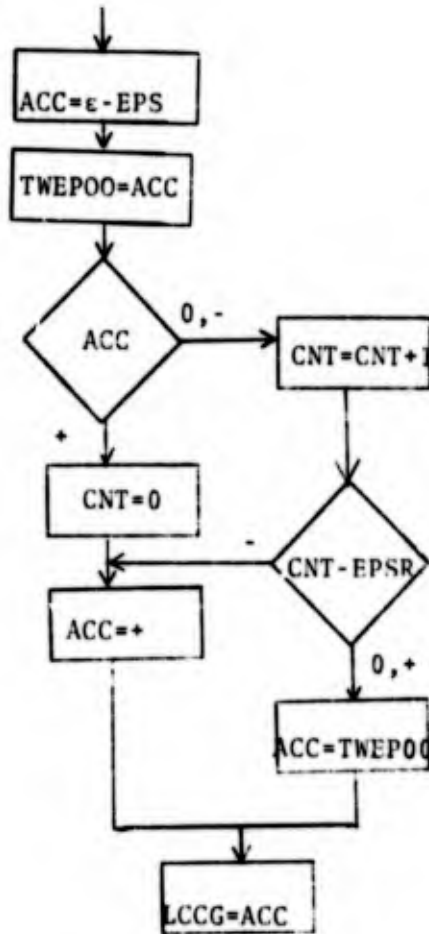
03FE	EFD1
03FF	D245

LEGEND:

ϵ \equiv Pilot Error (radial)
 EPS \equiv Size of Coincidence Window (mr)
 EPSR \equiv No. of Computation Cycles coincidence must be maintained

If LCCG > 0, gun fire signal is inhibited.

FLOW DIAGRAM



Bauman/Kravec "Time in Coincidence" Test

Figure C-3